Journal of Biomedical Optics 8(3), 432–439 (July 2003)

High-resolution multiphoton tomography of human skin with subcellular spatial resolution and picosecond time resolution

Karsten König
Iris Riemann
University of Jena
Laser Microscopy Division
D-07740 Jena, Germany
E-mail: kkoe@mti-n.uni-jena.de

Abstract. High-resolution four-dimensional (4-D) optical tomography of human skin based on multiphoton autofluorescence imaging and second harmonic generation (SHG) was performed with the compact femtosecond laser imaging system *DermaInspect* as well as a modified multiphoton microscope. Femtosecond laser pulses of 80 MHz in the spectral range of 750 to 850 nm, fast galvoscan mirrors, and a time-correlated single-photon counting module have been used to image human skin *in vitro* and *in vivo* with subcellular spatial and 250-ps temporal resolution. The nonlinear induced autofluorescence originates from naturally endogenous fluorophores and protein structures such as reduced nicotinamide adenine dinucleotide phosphate, flavins, collagen, elastin, porphyrins, and melanin. Second harmonic generation was used to detect collagen structures. Tissues of patients with dermatological disorders such as psoriasis, fungal infections, nevi, and melanomas have been investigated. Individual intratissue cells and skin structures could be clearly visualized. Intracellular components and connective tissue structures could be further characterized by fluorescence excitation spectra, by determination of the fluorescence decay per pixel, and by fluorescence lifetime imaging. The novel noninvasive multiphoton autofluorescence-SHG imaging technique provides 4-D (x,y,z,τ) optical biopsies with subcellular resolution and offers the possibility of introducing a high-resolution optical diagnostic method in dermatology. [DOI: 10.1117/1.1577349]

Keywords: multiphoton; skin; optical tomography; femtosecond lasers; fluorescence lifetime; optical biopsy.

Paper MM-07 received Nov. 6, 2002; revised manuscript received Jan. 16, 2003; accepted for publication Jan. 31, 2003.

1 Introduction

In contrast to the standard technique of determining the histopathology of mechanically removed tissue, noninvasive three-dimensional (3-D) optical diagnostics has the advantage of (1) providing a painless diagnostic method without tissue removal, (2) rapid access to information, (3) examination under natural physiological (*in vivo*) conditions, and (4) the possibility of long-term studies on the same tissue area, including *in vivo* drug screening.

Human skin has to be considered as an optically turbid media where the incident light photons undergo multiple scattering before absorption occurs. Backscattered photons may leave the skin (diffuse reflection). Absorbed photons can induce a weak autofluorescence based on naturally occurring endogenous fluorescent biomolecules such as flavins, reduced nicotinamide adenine dinucleotide phosphate [NAD(P)H] coenzymes and metal-free porphyrins as well as components of lipofuscin, collagen, elastin, and keratin (Table 1). Autofluorescence and reflection can be used to perform optical imaging of the structural components of tissues. In order to obtain high-resolution depth-resolved (3-D) images, methods with the capability of optical sectioning have to be applied, such as the confocal detection method.[1]

Confocal laser scanning microscopes have been used to perform optical sectioning of human skin either in the reflection[2–4] or in the fluorescence mode.[5] *In vivo* confocal autofluorescence images were obtained at depths down to 85 μm using excitation wavelengths at 365 and 488 nm.[5] One-photon fluorescence excitation has, however, the disadvantages of low light penetration depth, out-of-focus photodamage, and out-of-focus photobleaching. In addition, multiple scattering reduces the information obtained in the confocal detection mode because of those scattered out-of-focus photons which are transmitted through the pinhole onto the detector. Furthermore, the photon collection efficiency is low, owing to spatial filtering by the pinhole.

These disadvantages can be overcome by multiphoton fluorophore excitation using near-infrared (NIR) femtosecond laser pulses and high numerical aperture (NA) objectives.[6] In the range of 700 to 1200 nm, the one-photon absorption coefficients and scattering coefficients of skin are low compared with the UV/visible spectrum, owing to the absence of effi-

1083-3668/2003/$15.00

Table 1 Spectral characteristics of endogenous skin fluorophores.

Fluorophore	Excitation Wavelength (nm)	Emission Wavelength (nm)	Fluorescence Lifetime (ns)
NAD(P)H	340	450 to 470	0.3 (bound to proteins: 2)
Flavines	370, 450	530	5.2 (pound to proteins: <1)
Elastin	300 to 340	420 to 460	0.2 to 0.4/0.4 to 2.5
Collagen	300 to 340	420 to 460	0.2 to 0.4/0.4 to 2.5
Melanin	UV/visible	440, 520, 575	0.2/1.9/7.9
Lipofuscin	UV/visible	570 to 590	Multiexponential

cient absorbers and because the strength of the Rayleigh scattering is inversely proportional to the fourth power of the illumination wavelength. Therefore, NIR intensities as high as a gigawatt per square centimeter can be applied without damage to tissues and fluorophores, and deep tissue imaging can be realized. Multiphoton excitation occurs in only a tiny intratissue focal volume, on the order of 1 fl or lower. Using a fast galvoscanner and a piezodriven objective positioner, the position of the multiphoton excitation volume can be changed in three directions to realize deep-tissue optical sectioning. By means of pinhole-free detectors in the descanned mode (fluorescence not transmitted through the scanners), fluorescence imaging at high photon collection efficiency can be realized. Blue-green emitting fluorophores such as NAD(P)H, which normally require UV excitation, can be imaged even in the dermis. It was predicted that diffraction-limited image resolution can be maintained for skin tissue of thicknesses up to 500 μm.[7]

Using a two-photon femtosecond laser scanning microscope, Masters et al.[8] detected the autofluorescence of human skin in depths down to 200 μm. Optical sectioning of animal and human skin by NIR femtosecond laser autofluorescence microscopy has been reported, for example, by So and Kim,[9] Masters et al.,[10] Hendriks and Lucassen,[11] König et al.,[12–15] and Peuckert et al.[16] Teuchner et al.[17] reported on femtosecond pulse excitation of melanin fluorescence. Multiphoton microscopes are normally not suitable for imaging of human skin. Here we report on a novel femtosecond laser scanning system for high-resolution multiphoton tomography of normal human skin and dermatological disorders with the capability of submicron spatial resolution and a 250-ps temporal resolution. The system allows the measurement of fluorescence decay kinetics per pixel and fluorescence lifetime imaging of optical sections by time-resolved single-photon counting (TRSPC).[18] The high-resolution imaging system is designed for use in dermatology and pharmaceutical research, including long-term *in vivo* drug screening.

2 Materials and Methods

2.1 *The System DermaInspect*

All components of the laser imaging system DermaInspect 110 are mounted on a transportable workstation (Fig. 1). The system, with a total dimension of $75\times120\times140$ cm^3, is considered a class 1M device according the new European laser safety regulations. It consists of the following three major modules[15]:

1. A compact, turnkey, solid-state, mode-locked 80-MHz titanium:sapphire laser (Ti:S) (MaiTai, Spectra Physics) with a tuning range of 750 to 850 nm, a maximum laser output of about 900 mW, and a 75-fs pulse width.
2. A scanning module, including a motorized beam attenuator and shutter; a laser power detection module and trigger module for the TCSPC unit; a fast *x,y* galvoscanner and piezodriven 40× focusing optics with NA 1.3 (oil, 140-μm working distance, WD) or 20× optics NA 0.9 (water, 1.2 mm WD); a photomultiplier tube (PMT) with a short rise time; and a module with a 0.17-μm glass window for *in vivo* skin studies.
3. A control module with power supplies; a single-photon counting board (SPC 730/830, Becker&Hickl Berlin); and image-processing hardware and software, including such features as online control of laser power and adjustment according to tissue depth, monodirectional and bidirectional scanning, line scan, and single-point illumination.

Fig. 1 Photograph of the multiphoton imaging tool DermaInspect 110 for 4-D autofluorescence and SHG imaging with intracellular spatial resolution and 250-ps temporal resolution.

The tissue phantoms for microscopy (TPM, Riemann Labortechnik, Jena, Germany) were placed in sterile microchambers with 0.17-μm-thick glass windows filled with 1% low-melting agarose. Intralipid 10 scattering particles and fluorescent microspheres of different sizes and different fluorescence spectra have been used to characterize the spatial and temporal resolution of the system.

2.2 *The Multiphoton Microscope*

A confocal laser scanning microscope (LSM 410, Zeiss) was modified to create a multiphoton microscope in such a way that (1) the optics were changed to obtain a high transmittance of 0.7 (800 nm), (2) an interface (JenLab GmbH, Jena, Germany) for introduction of a femtosecond laser source was provided, and (3) a special baseport unit equipped with a fast PMT, CCD camera, and spectrometer was created.

2.3 *Biopsies and in Vivo Measurements*

Biopsies were obtained from patients with a variety of diseases, including psoriasis, nevi, melanomas, and dermatomycosis. For transportation and safe measurement, the samples were placed in sterile biopsy chambers for microscopy (MiniCeM-biopsy, JenLab GmbH) consisting of silicon with 4-mm holes and 0.17-μm-thick glass windows on both sides for inverted and upright imaging. Isotonic sodium chloride (NaCl) solution was used to prevent drying. The measurements occurred within 1 h after excision. Optical sectioning of *in vivo* Caucasian human skin (type II) of a male volunteer 41 years old and a female volunteer 33 years old was carried out on the lower forearm, which was placed on an arm holder.

2.4 *Time-Resolved Autofluorescence Measurements*

Using the TCSPC method, single fluorescence photons have been counted with a fast PMT (transient time spread 150 ps) equipped with short-pass Schott BG 39 filters. The system allows count rates of more than 10^6 photons per second at 80 MHz. Typically, the two-photon excited autofluorescence of skin at moderate laser powers provided count rates of about 100,000 photons per second. The PMT signal was synchronized with the *x,y,z* beam position calculated from signals of the galvoscanner and the piezodriven objective. This information was used to provide spatially resolved autofluorescence decay curves per pixel; to fit these curves by a mono-, bi-, or three-exponential approach; and to calculate mean fluorescence lifetimes per pixel or per region of interest. The calculated mean fluorescence lifetimes were depicted as color-coded τ-images.

3 Results

3.1 *Alignment*

Tissue phantoms for microscopy have been used for proper beam alignment and to test the imaging system by the determination of point spread functions (PSF) dependent on the intratissue depth of the excitation volume and the fluorescence wavelength, and to probe the temporal resolution. We measured a lateral PSF width of 0.4 to 0.6 μm and an axial PSF of 1.2 to 2.0 μm during optical sectioning between 0 and 100 μm depth in spite of scattering material (0 to 1%) and a temporal resolution of about 250 ps.

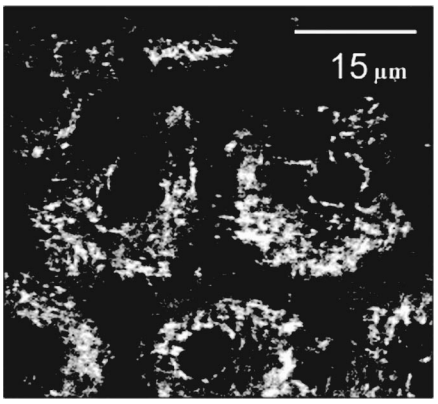

Fig. 2 High-resolution *in vivo* multiphoton autofluorescence image of seven cells in the stratum spinosum at about a 45-μm depth in the left forearm of a female volunteer (laser excitation, 760 nm).

Alignment of the skin surface occurred typically during fast scanning (1 s per frame at $512\times512=262{,}144$ pixels) and detection of the strong autofluorescence of the outermost tissue layer, the stratum corneum. Typically, a mean power of 2 mW was chosen, which corresponds to a pulse energy of 25 pJ. In order to obtain high-contrast images, the scan speed was reduced to 8 s per frame, which corresponds to a mean beam dwell time per pixel of 30 μs. The *z*-position was varied in steps of 1, 5, or 10 μm to a deeper position. For in-depth imaging, the incident laser power was increased. When imaging at a tissue depth of 100 μm, typically the incident mean laser power was chosen to be 20 mW (750 nm).

3.2 *Optical Sectioning of an Area within the Human Forearm*

Figure 2 demonstrates a high-resolution *in vivo* autofluorescence image of seven cells deep in the epidermis within the stratum spinosum. The intracellular dark areas reflect the nonfluorescent nuclei. Two-photon excitation at 760 nm resulted in NAD(P)H fluorescence. The reduced coenzymes NAD(P)H are mainly located in mitochondria. As is obvious from this figure, even single autofluorescent mitochondria can be imaged deep into the tissue. The right cell depicted in the image exhibits multiple nuclei that are most likely due to ongoing cell devision.

Figure 3 shows images at different tissue depths separated by 5 μm out of a stack of optical sections of a male volunteer using 750-nm femtosecond laser pulses. Single cells, cellular components, extracellular structures, and transitions between tissue layers could be clearly recognized by nonlinear NIR-excited autofluorescence. In particular, the autofluorescence image of connective tissue from a depth of 80 μm demonstrated excellent in-depth resolution. The stratum corneum, with its fluorescent component keratin, exhibited a strong autofluorescence when excited within the tuning range of 750 to 850 nm. Within the broad excitation band, maxima at 750 nm and at around 820 nm have been detected in a small skin area of one volunteer. However, excitation spectra varied among different locations within this cornified tissue layer. The cell borders of the hexagonal-shaped corneocytes with a mean cell diameter of 36 ± 15 μm often induced the strongest fluores-

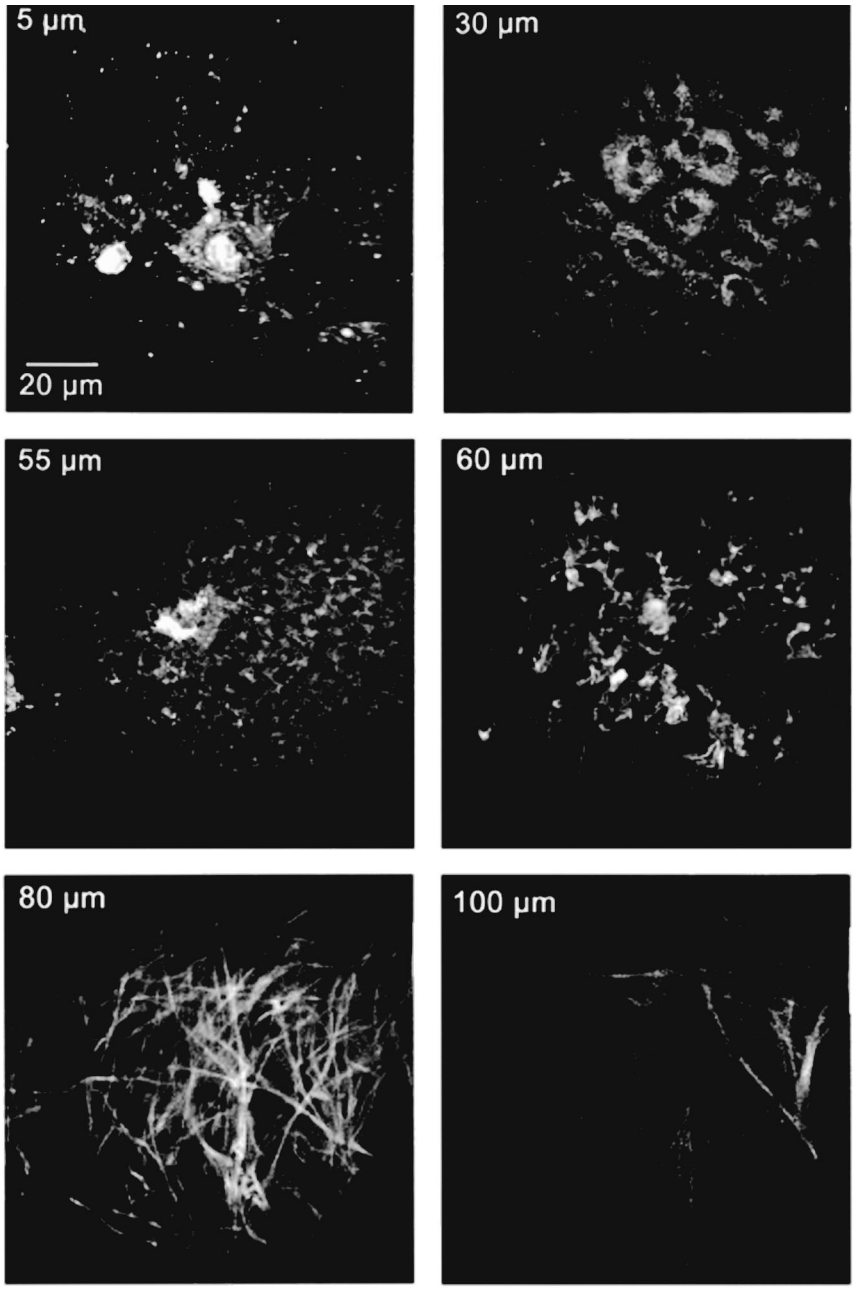

Fig. 3 *In vivo* optical tomography of the forearm of a male volunteer. The image at 5 μm shows fluorescent structures of the stratum corneum whereas the images at 30, 55, and 60 μm reflect fluorescent epidermal organelles. The images at 80 and 100 μm show connective structures in the dermis.

cence of the tissue. The fluorescence pattern on the skin surface was interrupted by nonfluorescent areas with a thickness of up to 100 μm, owing to epidermal ridges. However, in the lower epidermal layers, the fluorescent borders (corneocytes) of these incisions were responsible for highly luminescent areas down to 50 μm or more. Hairs appeared as highly fluorescent structures. The thickness of the stratum corneum in the area of interest (lower forearm) was found to be 10 to 15 μm (female) and 15 to 20 μm (male).

The transition to the stratum granulosum was detected by the occurrence of living cells with a different cell shape, a fluorescent cytoplasm, and nonfluorescent nuclei. In general, the autofluorescence of this tissue layer appeared of low contrast and more diffuse, owing to the coexistence of living and dead fluorescent cells. A typical thickness of about 10 μm for this tissue layer was found.

Within the stratum spinosum, the single cells and cellular compartments could be clearly seen by strong-fluorescent granula in the cytoplasm and the borders of the large, round, nonfluorescent nuclei. The cell diameter decreases with increasing tissue depth and was found in the upper part of this layer to be 26 ± 3 μm and in the deepest cell layer 16 ± 4 μm. Also, the ratio between the volume of the cytoplasm

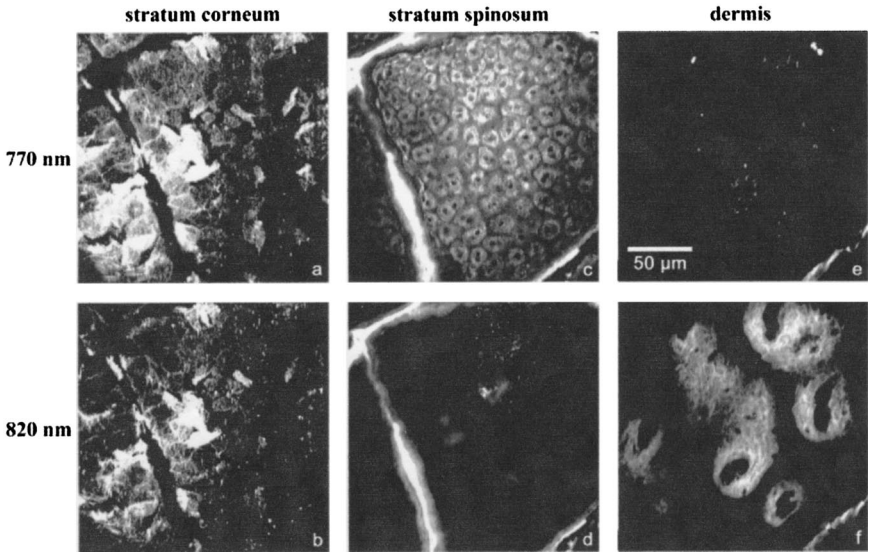

Fig. 4 *In vivo* optical tomography in dependence on excitation wavelength. Signals in the dermis at 820-nm excitation are mainly due to SHG radiation (a,c,e: 770 nm; b,d,f: 820 nm, female volunteer).

and the volume of the nuclei decreased. Sometimes cells with two nuclei were found.

The single innermost cell layer of the epidermis, the stratum basale, was determined by cuboidal cells with higher fluorescence intensity than living cells in the upper layers. Very likely these are the basal cells that can be differentiated and that migrate toward the skin surface. Within these cells, strong fluorescent granula in the upper part of the perinuclear region have been detected. The basal cells had the lowest diameter of the epidermal cells, with 9 ± 1 μm, and the lowest ratio of cytoplasm to nuclei volume. During optical sectioning, the basal cells occurred as a circular cluster around the tip of a papilla.

The transition between epidermis and corium (cutis) was determined by the distribution of the papillae. Typically this junction was found at a depth of 55 to 70 μm for the female and 70 to 100 μm for the male volunteers. Connective tissue, in particular, single fluorescent long fibers with a thickness of less than 1 μm, could be clearly visualized. These highly fluorescent structures are properly single elastin fibers.

The images in Fig. 4 reflect the dependence on excitation wavelength. The figure shows some *in vivo* images at 770 and 820 nm out of a wavelength stack. The laser was tuned from 750 to 850 nm in steps of 10 nm. In general, the fluorescence intensity increased when the laser was tuned to short wavelengths. This is in accordance with the absorption behavior of the coenzymes NAD(P)H and flavins. However, optical sectioning with excitation wavelengths larger than 780 nm through the junction of the epidermis and dermis and within the dermis resulted in an additional source of luminescence and its detection. This luminescence is based on a second harmonic generation (SHG) of collagen. Therefore, the signal obtained from the dermis was found to be a combination of two-photon excited autofluorescence and of SHG formation at half the excitation wavelength. The SHG part was detected by determination of the emission wavelength using a variety of narrow bandpass filters and by tuning the excitation wavelength. It was clearly found that the signal possesses a short spectral bandwidth in contrast to fluorescence. In addition, a component with a short (picosecond) decay time was detected in the dermal region. The reason the SHG signal could be measured only at excitation wavelengths above 780 nm is due to the reduced transmission of the short-pass filters in the ultraviolet. In order to further verify that SHG signals are generated in the dermis, 10-μm-thick cryosections of a biopsy of Caucasian skin were investigated at 820 nm. No SHG signal was detected in the layers of the epidermis. However, a strong blue signal between 400 and 420 nm was detected in dermal collagen.

In addition to the imaging of autofluorescence intensity, *in vivo* fluorescence decay kinetics per pixel have been measured. From these large amounts of data two major fluorescence lifetime components have been determined. The shorter one has a time within the response time of the detector and is most likely due to the SHG signal in the UV and blue spectral range and a small amount of scattered light that was able to transmit the filters. The long component is due to autofluorescence. Its lifetime has been calculated and depicted as a false-color fluorescence lifetime image. Typically the fluorescence lifetime of an intratissue cell was found to be on the order of 1.8 to 2.4 ns. Figure 5 shows two optical sections out of a stack of 3-D τ-maps. One image shows the autofluorescence lifetime image of the stratum corneum. The histogram of the fluorescence lifetime distribution (right upper corner of the image) shows a maximum at about 1.9 ns. The lifetime image is dominated by yellow pixels because of the false color table chosen in which yellow corresponds to 1.78 to 1.94 ns. A particular decay curve of a part of the cell border is shown in the lower part. Deconvulation resulted in the calculation of a long-lived component with a mean fluorescence lifetime of 1.85 ns. In contrast, the lower image taken at a depth of 50 μm within the stratum spinosum shows a histogram maximum of about 2.4 ns and a single fluorescence decay curve of a pixel in the perinuclear region within an organelle that might be mitochondria. The biexponential deconvulation shows a component with a relatively long fluorescence life-

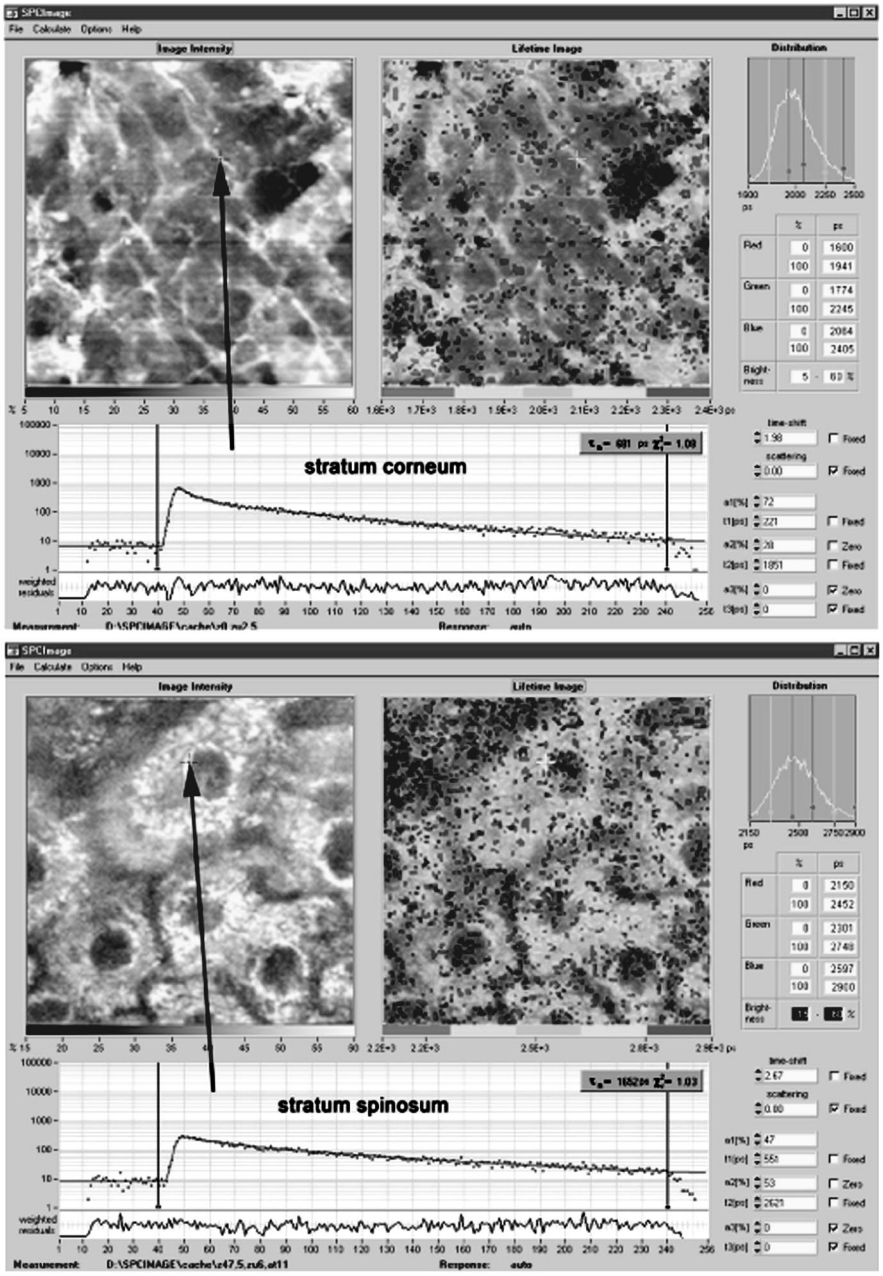

Fig. 5 *In vivo* autofluorescence lifetime images of stratum-corneum (upper panel, 5 μm) and stratum spinosum (lower panel, 50-μm tissue depth).

time of 2.7 ns. Mitochondrial protein-bound NAD(P)H has typical lifetimes in the range of 2 to 3 ns, in contrast to NAD(P)H in solution, which has picosecond lifetimes (Table 1).

These *in vivo* studies on normal human skin demonstrate the capability of four-dimensional autofluorescence imaging in deep tissue with a subcellular resolution in the range of 1 μm and picosecond temporal resolution. Time-correlated single-photon counting allows the measurement of intratissue fluorescence decay kinetics and the calculation of mean fluorescence lifetimes. In addition, it supports the detection of second harmonic generation in the tissue depth by the detection of a short luminescence component limited by the temporal resolution of the detector (in this experimental setup, 250 ps). The process of SHG occurs immediately, in contrast to fluorescence with its typical lifetime in the nanosecond range.

3.3 *Imaging of Dermatological Disorders*

Sixty biopsies of patients with different dermatological disorders that included psoriasis, warts, fungal infections, nevi, and benign and malignant skin cancers have been investigated by multiphoton-excited autofluorescence imaging. The pattern and intensity of the autofluorescence differed clearly from surrounding normal tissue.

In the images of the patient with trichophytosis (dermatomycosis) hexagonal-shaped strong fluorescent corneocytes

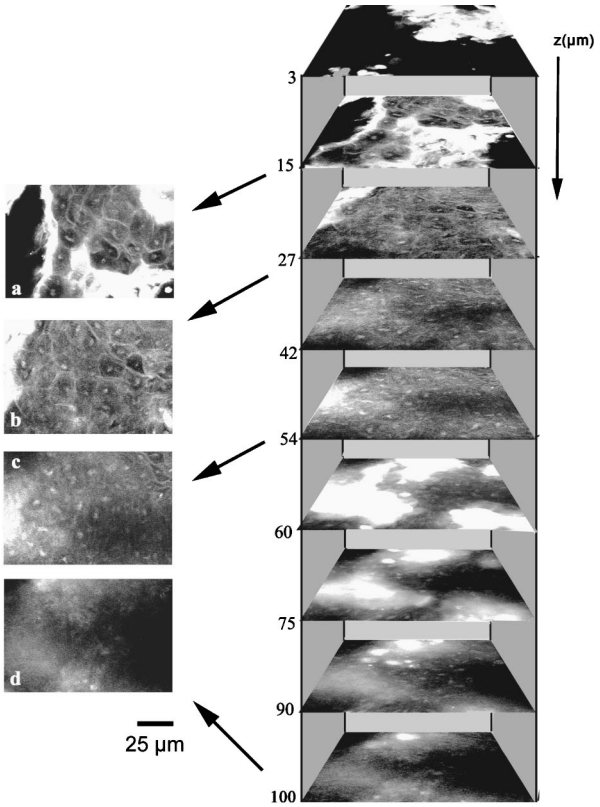

Fig. 6 Autofluorescence images of skin with fungal infection (trichophytosis).

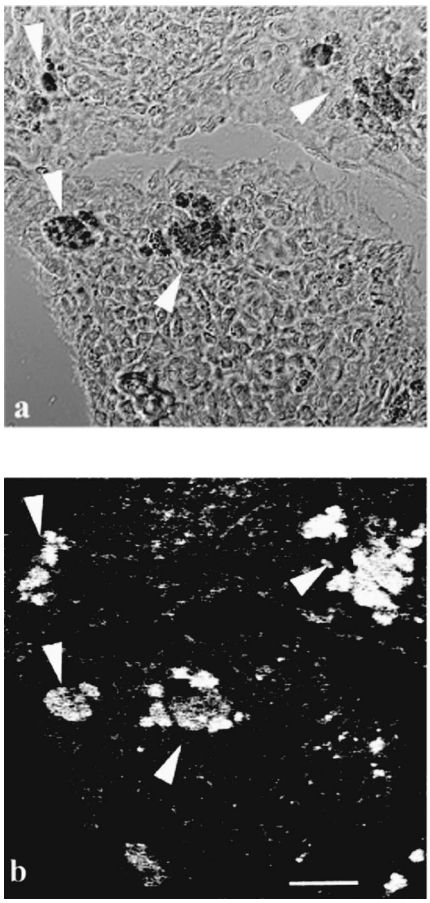

Fig. 7 Multiphoton autofluorescence image and transmission image of a pigmented cryosection demonstrating multiphoton-excited luminescence of melanin.

with a mean diameter of 90 ± 20 μm have been detected in depths down to 80 μm. It is interesting that these corneocytes revealed strong fluorescent nuclei compartments. Such nuclei compartments can arise during hyperkeratosis. Within this 90-μm-thick tissue layer, the fluorescence intensity increased with increasing tissue depth (Fig. 6). NIR femtosecond laser pulses can be also used to excite intense fluorescence of the melanin pigment (Fig. 7). Pigmented and nonpigmented areas could be clearly differentiated. In the case of a melanocytic compound nevi, the intensity of this autofluorescence was significantly increased. This was based on strongly fluorescent cells in all tissue layers, from the stratum granulosum down to the dermal–epidermal junction. The fluorescence from these cells arose from fluorescent granula.

In the case of a malignant melanoma, no clear transitions between the different tissue layers were recognized (Fig. 8). Clusters of highly fluorescent cells appeared. In tissue depths of 40 μm and more that were measured, the fluorescence intensity was so large that the fluorescence excitation power could be reduced by 30 to 50%. As indicated by the autofluorescence images and transmission images of cryosections of pigmented skin from patients with melanocytic nevi and superficially spreading melanomas, the pigmented dark compartments that contain melanin revealed the strongest fluorescence compared with nonpigmented areas.

4 Discussion

Multiphoton tomography of skin by sophisticated versatile bioinstrumentation based on intense femtosecond NIR laser beams at subnanojoule pulse energy provides a high-resolution view of the different layers of the skin. Using subfemtoliter excitation volumes and NIR excitation light in combination with *x*,*y*,*z* scanning, three-dimensional imaging of dermatological disorders and *in vivo* drug screening at subcellular intratissue resolution becomes possible. Using the additional contrast-enhancing mechanism of τ-mapping, the capability can even be enhanced to 4-D imaging (space and time). In-depth lifetime imaging provides the possibility of obtaining further information on the type of fluorophore and its intratissue distribution and microenvironment as well as on the type of luminescence (fluorescence or SHG). In order to obtain additional information on scattering processes and the true path length of backscattered in-depth photons, faster detectors are required. In the time period of 250 ps, which represents the current temporal resolution of the system, intratissue photons travel 5 cm, or a distance 500 times the thickness of the epidermis.

Autofluorescence and SHG imaging by NIR multiphoton excitation provides a better resolution than optical coherence tomography (OCT) and enhanced in-depth information compared with confocal imaging techniques. In addition, functional imaging becomes possible by autofluorescence detection owing to the fluorescence excitation of the biosensor NAD(P)H in its reduced state and the measurement of the

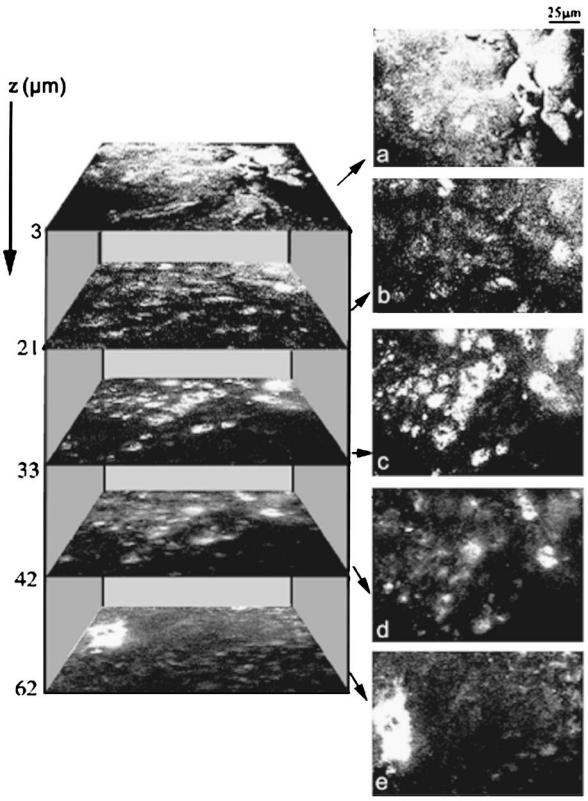

Fig. 8 *Ex vivo* optical sectioning through a superficial spreading melanoma. Five images at 3, 21, 33, 42, and 62 μm depth out of a stack are characterized by bright fluorescent granula.

fluorescence decay kinetics that are dependent on the microenvironment, etc. It is interesting that intense femtosecond laser pulses in dermal collagen generate radiation at half the incident wavelength by second harmonic generation. Although the second harmonic (SH) photons exit the focal point in the same direction as the exciting light, some of these UV/blue photons can be detected at the skin surface owing to multiple scattering. Spectral imaging would be helpful in quantifying the SH contribution to the overall backscattered luminescence. Further basic research and clinical studies have to be performed to evaluate the enormous potential of this technique and system of multiphoton autofluorescence imaging in dermatology and drug screening, and to use multiphoton-induced emission of melanin for a possible diagnosis of melanoma.

Acknowledgments

The authors wish to thank Prof. Wollina, Prof. Elsner, and Dr. Fünfstück for discussions regarding dermatological disorders and for providing biopsies; Dr. Peter Fischer (JenLab GmbH, Jena, Germany) and Jens Vogel and coworkers (Vogel AT GmbH, Dorndorf, Germany) for technical support; and Christiane Peuckert, Annette Reif, and Volker Ulrich for measurements on biopsies. This work was in part supported by BMBF grant 01ZZ0105.

References

1. *Handbook of Biological Confocal Microscopy*, J. B. Pawley, Ed., Plenum, New York (1995).
2. M. Rajadhyaksha, S. Gonzalez, J. M. Zavislan, R. R. Anderson, and R. H. Webb, ''*In vivo* confocal laser scanning laser microscopy of human skin II: advances in instrumentation and comparison with histology,'' *J. Invest. Dermatol.* **113**, 293–303 (1999).
3. M. Rajadhyaksha, R. Rox Anderson, and R. H. Webb, ''Video-rate confocal scanning laser microscope for imaging human tissues *in vivo*,'' *Appl. Opt.* **38**, 2105–2115 (1999).
4. C. Peuckert, I. Riemann, U. Wollina, and K. König, ''Remission microscopy with NIR femtosecond laser pulses for 3D *in vivo* imaging of human skin,'' *Cell. Molec. Biol.* **46**, abstract 117 (2000).
5. B. R. Masters, ''Three-dimensional confocal microscopy of human skin *in vivo*: autofluorescence of human skin,'' *Bioimaging* **4**, 13–19 (1996).
6. W. Denk, J. H. Strickler, and W. W. Webb, ''Two-photon laser scanning microscopy,'' *Science (Washington, DC, U.S.)* **248**, 73–76 (1990).
7. X. Deng, X. Gan, and M. Gu, ''Multiphoton fluorescence microscopic imaging through double-layer turbid tissue media,'' *J. Appl. Phys.* **91**, 4659–4665 (2002).
8. B. R. Masters, P. T. C. So, and E. Gratton, ''Multiphoton excitation fluorescence microscopy and spectroscopy of *in vivo* human skin,'' *Biophys. J.* **72**, 2405–2412 (1997).
9. P. T. C. So and H. Kim, ''Two-photon deep tissue *ex vivo* imaging of mouse dermal and subcutaneous structures,'' *Opt. Express* **3**, 339–350 (1998).
10. B. R. Masters, P. T. C. So, and E. Gratton, ''Multiphoton excitation microscopy of *in vivo* human skin,'' *Ann. N.Y. Acad. Sci.* **838**, 58–67 (1998).
11. R. F. M. Hendriks and G. W. Lucassen, ''Two photon fluorescence microscopy of *in vivo* human skin,'' *Proc. SPIE* **4164** (1999).
12. K. König, ''Review: multiphoton microscopy in life sciences,'' *J. Microsc.* **200**, 83–104 (2000).
13. K. König, ''Laser tweezers and multiphoton microscopes in life sciences,'' *Histochem. Cell. Biol.* **114**, 79–92 (2000).
14. K. König, C. Peuckert, I. Riemann, and U. Wollina, ''Non-invasive 3D optical biopsy of human skin with NIR-femtosecond laser pulses for diagnosis of dermatological disorders,'' *Cell. Mol. Biol.* **46**, abstract 117 (2000).
15. K. König, U. Wollina, I. Riemann, C. Peuckert, K. J. Halbhuber, H. Konrad, P. Fischer, V. Fünfstück, T. W. Fischer, and P. Elsner, ''Optical tomography of human skin with subcellular spatial and picosecond time resolution using near infrared femtosecond laser pulses,'' *Proc. SPIE* **4620**, 190–201 (2002).
16. C. Peuckert, I. Riemann, and K. König, ''Two photon induced autofluorescence of *in vivo* human skin with femtosecond laser pulses—a novel imaging tool of high spatial, spectral and temporal resolution,'' *Cell. Mol. Biol.* **46**, abstract 179 (2000).
17. K. Teuchner, W. Freyer, D. Leupold, A. Volkmer, D. J. Birch, P. Altmeyer, M. Strucker, and K. Hoffmann, ''Femtosecond two-photon excited fluorescence of melanin,'' *Photochem. Photobiol.* **70**, 146–151 (1999).
18. W. Becker, A. Bergmann, K. König, and U. Tirlapur, ''Picosecond fluorescence lifetime microscopy by TCSPC imaging,'' *Proc. SPIE* **4262**, 414–419 (2001).